Journal of the Ceramic Society of Japan 117 [12] 1302-1305 2009 **Paper**

Nanostructure control of liquid-phase sintered Si_3N_4 ceramics by spark plasma sintering

Mikinori HOTTA[†,‡] and Junichi HOJO

Department of Applied Chemistry, Faculty of Engineering, Kyushu University, 744, Motooka, Nishi-ku, Fukuoka 819−0395

Submicron-sized α-Si_3N_4 and nanosized amorphous Si_3N_4 powders were sintered by spark plasma sintering at 1700°C for holding times of 60 to 120 s at heating rates of 1.7 to 6.1°C/s with Y_2O_3 and Al_2O_3 sintering additives. The nanostructure control of liquid-phase sintered Si_3N_4 ceramics was achieved by selecting optimum heating schedules such as temperature, holding time and heating rate. Fully dense nanostructured β-Si_3N_4 ceramics with grain size of 150 nm were prepared using nanosized amorphous Si_3N_4 starting powder. The transformation to β-phase in Si_3N_4 ceramics obtained from the nanosized amorphous Si_3N_4 powder was more greatly accelerated than that from submicron-sized α-Si_3N_4 powder.

Key-words : Silicon nitride, Spark plasma sintering, Nanostructure, Heating schedule, Densification, Phase transformation

[Received May 25, 2009; Accepted October 15, 2009]

1. Introduction

Silicon nitride (Si_3N_4) is difficult to densify without sintering additives because of its strong covalent bonding and low self-diffusion coefficients of Si and N. By adding sintering additives such as Y_2O_3 and Al_2O_3, liquid phase forms, resulting in fully dense Si_3N_4 ceramics. The grain morphology and grain boundary phase in the resultant Si_3N_4 ceramics affect the mechanical and thermal properties. In general, mechanical strength increases with decreasing grain size. The excellent fracture toughness of Si_3N_4 ceramics is achieved by the microstructure consisting of elongated β-Si_3N_4 grains with high aspect ratio.

Spark plasma sintering (SPS) technique can heat specimens rapidly, because the pulsed direct current used in this technique passes through a die and punch rods made of graphite.[1] Therefore, the time required for sintering can be shortened, thus resulting in retardation of grain growth during sintering. Furthermore, low-sinterable materials such as Al_2O_3, Si_3N_4, TiN, SiC, SiAlON and composites have been fabricated as high-density by SPS.[2)–11] From these features of SPS technique, it will be possible to control the microstructure of fully dense Si_3N_4 ceramics. This technique is often called by other name such as pulse electric current sintering (PECS),[3),6),8] field-assisted sintering technique (FAST)[7] and plasma-assisted sintering (PAS),[4] because the generation of spark discharge and/or plasma during SPS process has not been verified. Many researchers have already reported on the sintering of Si_3N_4 powders using SPS technique. Schneider et al.[4] have prepared fully dense Si_3N_4 ceramics, consisting of fine equiaxed α-Si_3N_4 grains from submicron-sized α-Si_3N_4 powder. Nishimura et al.[5] have revealed to form a microstructure with homogeneous nanosized grains using fine β-Si_3N_4 powder. Suganuma et al.[6] have studied the sintering behavior of submicron-sized α-Si_3N_4 powder and obtained fully dense Si_3N_4 ceramics with fine equiaxed grains.

† Corresponding author: M. Hotta; E-mail: hotta@jwri.osaka-u.ac.jp

‡ Present address: Joining and Welding Research Institute, Osaka University, Osaka 567-0047

The purpose of this work is to optimize heating schedule for the densification and inhibition of grain growth in Si_3N_4 ceramics using rapid heating of SPS technique, and is to prepare nanostructured Si_3N_4 ceramics using nanosized amorphous Si_3N_4 powder and SPS technique.

2. Experimental procedure

α-Si_3N_4 commercial powder (SN-E10 grade, β-phase: < 5%, total oxygen content: 1.2 mass%, Ube Industries, Ltd.) was used as starting material. SEM analysis of this powder confirmed that the average size of the particle was 170 nm (number mean diameter via SEM in **Fig. 1**). The high degree of particle agglomeration with a size in the range of 400 to 500 nm was observed in α-Si_3N_4 powder. Nanosized amorphous Si_3N_4 powder was also used as starting material instead of α-Si_3N_4 commercial powder. The nanosized amorphous powder was synthesized by a vapor phase reaction from $SiCl_4$ and NH_3 gases. The particles had spherical shape, and the average size of the particles was 80 nm (number mean diameter via SEM). The total oxygen content of the nanosized amorphous Si_3N_4 powder was 4.8 mass%. As sintering additives, 6 mass% Y_2O_3 (UU–HP grade, average par-

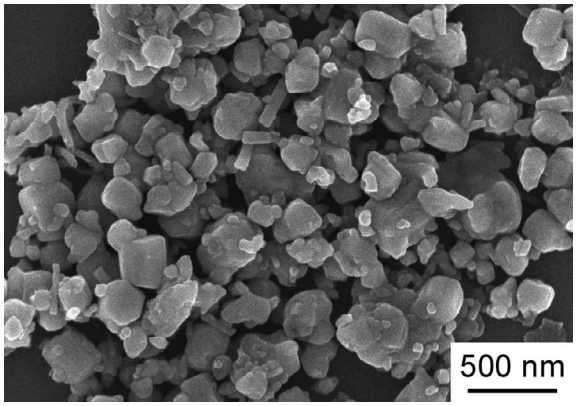

Fig. 1. SEM micrograph of submicron-sized α-Si_3N_4 starting powder.

ticle size: 300 nm, Shin-Etsu Chemical Co., Ltd.) and 2 mass% Al_2O_3 (AKP–20 grade, α-phase, average particle size: 500 nm, Sumitomo Chemical Co., Ltd.) powders were added to Si_3N_4. These powders were mixed with ethanol, dried and then passed through a sieve with pore-opening size of 300 μm. The mixed powder was compacted into graphite die and sintered by SPS (SPS–515S, SPS SYNTEX INC.) at temperatures of 1700 to 1800°C for holding times of 60 to 120 s in N_2 atmosphere at a pressure of 30 MPa. The heating rates were 1.7 to 6.1°C/s and the cooling rate was about 10°C/s. Pulsed direct current (pulses of 60 ms on/10 ms off) was applied. The sintering temperature on the surface of the die was measured by an optical pyrometer. Linear shrinkage of the powder compacts during the SPS process was continuously monitored by displacement of the punch rod. The densities of the specimens were measured by the Archimedes method. The phase transformation from α- to β-Si_3N_4 was evaluated using X-ray diffractometry (XRD; MiniFlex, Rigaku Corp.) with Cu Kα radiation for the sintered specimen. The content ratio of the α- and β-Si_3N_4 phases in the sintered Si_3N_4 bodies was determined from the peak intensities using equation proposed by Gazzara and Messier.[12] The specimens were polished with 3 μm diamond slurry, and then etched by plasma in a mixture of CF_4 and O_2 gases. The etched surfaces were observed by scanning electron microscopy (SEM; S–5200, JEOL Ltd.). The average grain size (number mean diameter) of the Si_3N_4 bodies was determined from average linear intercept length of 100 grains in the SEM images of the etched surfaces.

3. Results and discussion

3.1 Optimization of heating schedule for nanostructured Si_3N_4 ceramics

Heating schedule was optimized for obtaining nanostructured Si_3N_4 ceramics using a submicron-sized α-Si_3N_4 commercial powder. **Figure 2** shows the displacement of the α-Si_3N_4 powder compact with increasing temperature from 1000 to 1800°C at a heating rate of 1.7°C/s during SPS process. The isothermal displacement at 1800°C up to 120 s is also shown in Fig. 2. The shrinkage of the compact started at approximately 1300°C and finished at 1800°C within 120 s. The relative density of the resultant Si_3N_4 body reached 99.3%. The α-phase ratio was 9%, indicating a great degree of α- to β-Si_3N_4 phase transformation. SEM micrograph of the Si_3N_4 body sintered at 1800°C for 120 s was shown in **Fig. 3**. The typical microstructure of Si_3N_4 ceramics with elongated grains was observed.

Figure 4 shows the shrinkage of the α-Si_3N_4 powder compact as a function of whole sintering time at various heating rates of 1.7 to 6.1°C/s and at 1700°C for a holding time of 120 s. The shrinkage of the powder compact started at about 1300°C, which was independent of heating rate. The rapid shrinkage was caused and the shrinkage was completed within a few minutes. The relative densities of the final specimens sintered at 1.7, 3.0 and 6.1°C/s were 99.4, 98.9 and 98.5%, respectively. The α-phase ratio was 52 to 55%, and slightly increased with increasing heating rate. A large number of equiaxed grains were formed in the Si_3N_4 body sintered at 1700°C for 120 s, whereas the large elongated grains were observed in the Si_3N_4 body prepared at 1800°C for 120 s as shown in Fig. 3. This suggested that the development of elongated grains and α-β phase transformation were significantly dependent on sintering temperature. The average grain size of all the Si_3N_4 bodies prepared at 1700°C for 120 s was almost the same, about 200 nm, when heating rate changed between 1.7 and 6.1°C/s.

Figure 5 demonstrates the SEM micrographs of Si_3N_4 bodies prepared at 6.1°C/s and at 1700°C for holding times of 60 and 120 s using α-Si_3N_4 powder. A large number of equiaxed grains were observed in both specimens. The grain size of the Si_3N_4

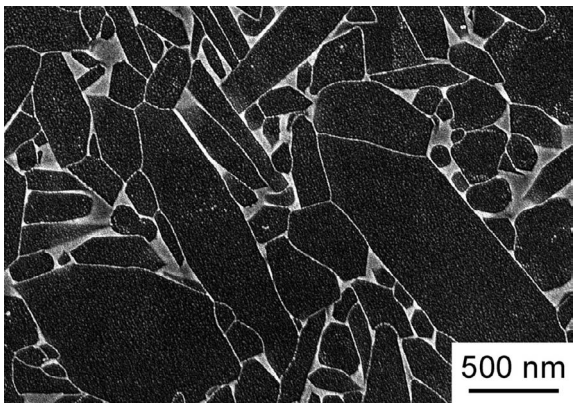

Fig. 3. SEM micrograph of the etched surface of Si_3N_4 body prepared using α-Si_3N_4 powder at a heating rate of 1.7°C/s, and at 1800°C for a holding time of 120 s.

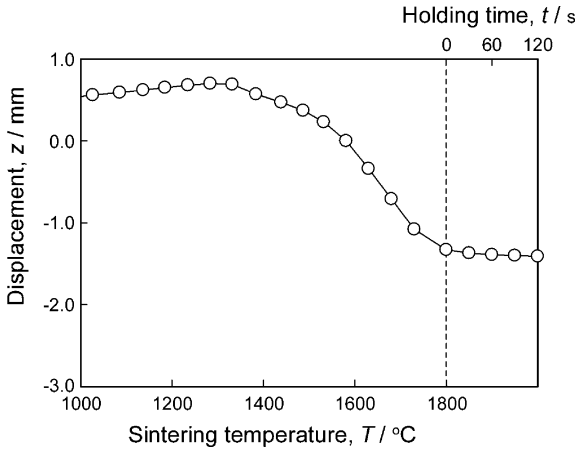

Fig. 2. Effect of sintering temperature on the displacement of α-Si_3N_4 powder compact at 1000 to 1800°C at a heating rate of 1.7°C/s, and the time dependence of isothermal displacement at 1800°C up to 120 s.

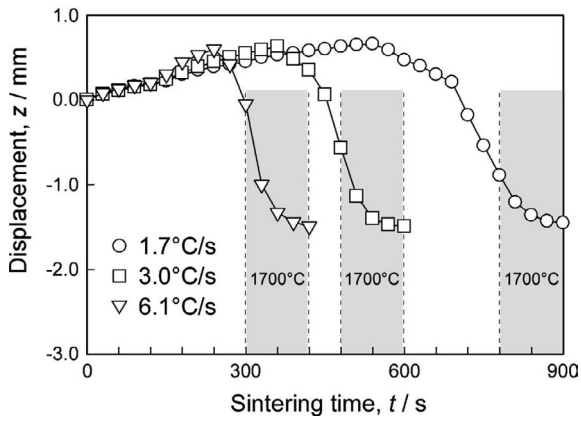

Fig. 4. Displacement of α-Si_3N_4 powder compact as a function of whole sintering time at different heating rates of 1.7 to 6.1°C/s up to 1700°C, and at 1700°C for a holding time of 120 s.

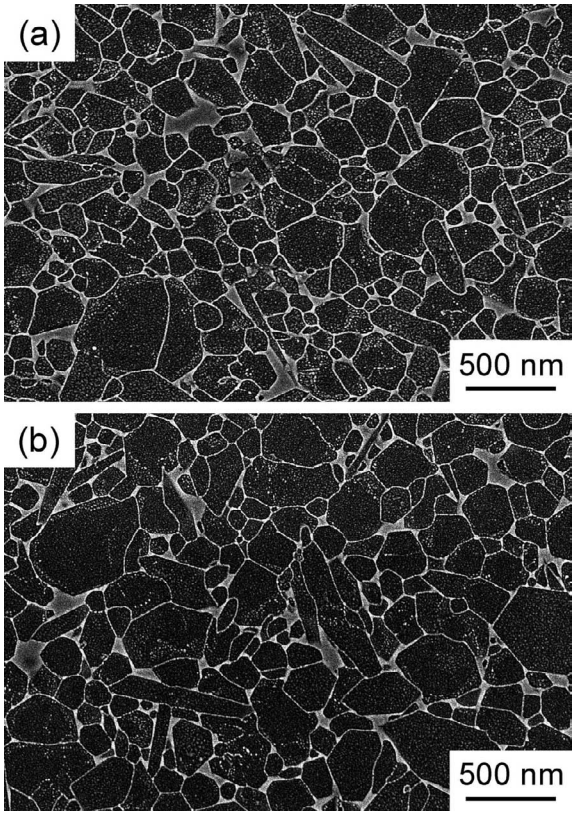

Fig. 5. SEM micrographs of the etched surface of Si_3N_4 bodies prepared using α-Si_3N_4 powder at 1700°C for holding times of 60 s (a), and 120 s (b).

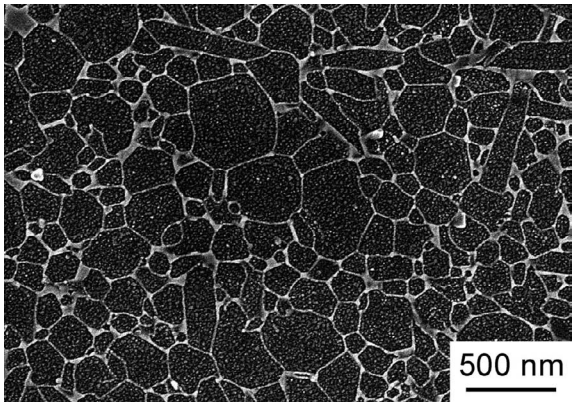

Fig. 6. SEM micrograph of the etched surface of Si_3N_4 body prepared using α-Si_3N_4 powder at 1700°C for 60 s and then cooled to 1500°C slowly at the rate of 3.3°C/s.

body sintered for 60 s was as small as 160 nm, but the full densification was not achieved, in which the relative density was 90.9%. When holding time increased from 60 to 120 s, the density improved to 98.5%, whereas the grain size increased from 160 to 200 nm. The α-phase ratio in the Si_3N_4 body decreased from 64 to 55% with increasing holding time from 60 to 120 s.

Consequently, heating schedule was changed as follows. The α-Si_3N_4 powder compact was heated at the rate of 6.1°C/s, at 1700°C for a holding time of 60 s and then cooled to 1500°C slowly at the rate of 3.3°C/s. The resultant specimen had high density, 97.1%. The microstructure of the Si_3N_4 body is shown

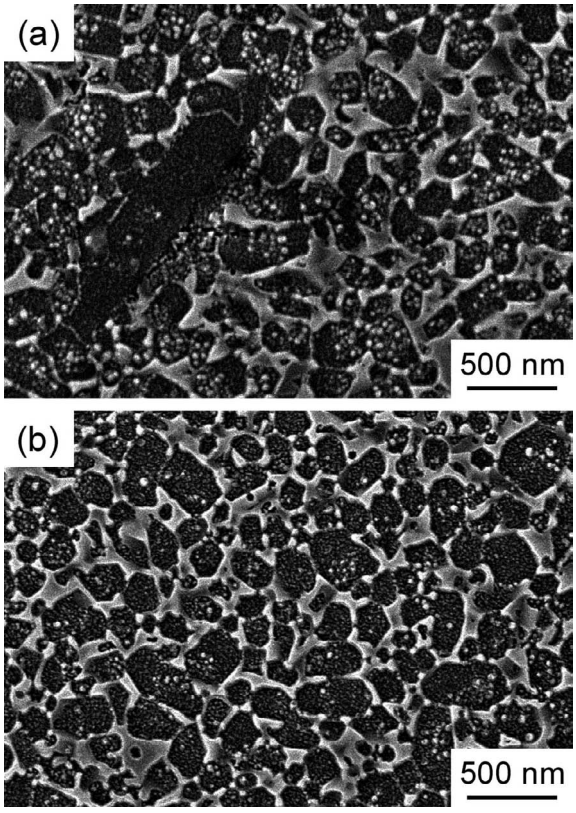

Fig. 7. SEM micrographs of the etched surface of Si_3N_4 bodies prepared using nanosized amorphous Si_3N_4 powder at 1700°C for 120 s (a), and at 1700°C for 60 s and then cooled to 1500°C slowly at the rate of 3.3°C/s (b).

in **Fig. 6**. The microstructure consisted mostly of equiaxed grains and the average size of the grains was 170 nm. The grain size was smaller than that of the Si_3N_4 body sintered at 1700°C for a holding time of 120 s. The α-phase ratio in the Si_3N_4 body was 61%. These results revealed that the grain growth can be inhibited by optimizing heating schedule. The grain size of 170 nm is equal to the particle size of the α-Si_3N_4 powder. Furthermore, it should be noted that the grain size is smaller than the size of agglomerates of the starting powder. This means that the agglomerates are dispersed during the liquid phase sintering process.

Schneider et al.[4] and Suganuma et al.[6] have reported that the phase transformation from α- to β-Si_3N_4 was delayed until the full densification was achieved for SPS, regardless of sintering conditions such as heating rate and atmosphere, although the phase transformation was concurrent with the densification for hot pressing. Additionally, the microstructure consisted of fine equiaxed grains until α-phase started to transform into β-phase for SPS. However, when the transformation from α- to β-phase was initiated, rapid grain growth occurred.[6]

3.2 Nanostructured Si_3N_4 ceramics from nanosized amorphous powder

Nanostructured Si_3N_4 ceramics were prepared using a nanosized amorphous Si_3N_4 powder and the optimized heating schedule which was possible to inhibit the grain growth. **Figure 7** shows the SEM micrographs of Si_3N_4 bodies prepared from nanosized amorphous Si_3N_4 powder. For a holding time of 120 s at 1700°C, a small number of elongated grains in length of about 1 μm were observed in fine-grained matrix (Fig. 7(a)). On the

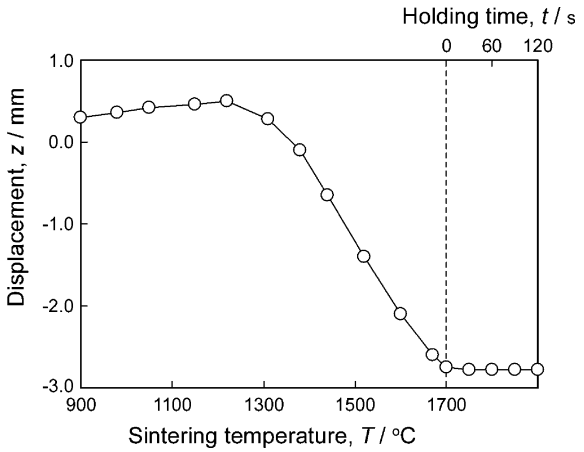

Fig. 8. Effect of sintering temperature on the displacement of nanosized amorphous Si_3N_4 powder compact at 900 to 1700°C at a heating rate of 1.7°C/s, and the time dependence of isothermal displacement at 1700°C up to 120 s.

other hand, when cooled slowly at 3.3°C/s after holding for 60 s at 1700°C, homogeneous microstructure with equiaxed grains was observed (Fig. 7(b)). The relative density of the Si_3N_4 sintered body was 97.1% and the average size of the grains was 150 nm, suggesting that the densification of Si_3N_4 ceramics was achieved with retarded grain growth. Nishimura et al.[5] have reported to fabricate β-Si_3N_4 bodies consisting of equiaxed grains with the size of 200 to 300 nm by SPS from β-Si_3N_4 powder with the size of 280 nm. The phase transformation from amorphous to crystalline β-phase was completed in both heating conditions in Fig. 7, whereas α-phase ratio of about 50% remained in Si_3N_4 bodies prepared using commercial α-Si_3N_4 powder. This implied that nanosized amorphous Si_3N_4 powder was more likely to transform into β-phase than submicron-sized α-Si_3N_4 powder. The displacement of nanosized amorphous Si_3N_4 powder compact with increasing temperature up to 1700°C at a heating rate of 1.7°C/s and the isothermal displacement at 1700°C up to 120 s are shown in **Fig. 8**. The shrinkage started at around 1250°C and ceased at 1700°C, which were lower starting and finishing temperatures of the shrinkage than those of submicron-sized α-Si_3N_4 powder as shown in Fig. 2. This might be due to smaller particle size and larger amount of total oxygen for nanosized amorphous Si_3N_4 powder. The phase transformation from α- to β-Si_3N_4 during hot pressing is commonly dependent on the densification.[13] The phase transformation of α-Si_3N_4 was concurrent with the densification for hot pressing, whereas the transformation proceeded after full densification for SPS.[6),14] Since the densification of nanosized amorphous Si_3N_4 powder was easier to proceed than that of submicron-sized α-Si_3N_4 powder, the transformation to β-phase might progress at lower temperature than that of submicron-sized α-Si_3N_4 powder. In addition, nanosized amorphous Si_3N_4 powder may be easy to dissolve in a liquid phase at a lower temperature during sintering, because nanosized amorphous Si_3N_4 is fine and unstable compared to submicron-sized α-Si_3N_4. Thus, a solution-reprecipitation process in nanosized amorphous Si_3N_4 arises at a lower temperature, resulting in the formation of fine grains and the transformation from amorphous to β-phase. It is also essential to select optimum conditions such as temperature, holding time and heating rate, because the microstructure of Si_3N_4 ceramics was largely dependent on heating schedule in SPS technique.

4. Conclusions

The effect of the heating schedule on densification of Si_3N_4 powder and microstructure of Si_3N_4 ceramics prepared by SPS technique through the liquid-phase sintering was investigated. Dense Si_3N_4 ceramics with inhibited grain growth during SPS process were obtained by selecting optimum heating schedules such as temperature, holding time and heating rate. Using nanosized amorphous Si_3N_4 powder as starting material, nanostructured β-Si_3N_4 ceramics consisting of equiaxed grains with 150 nm in diameter were prepared by SPS technique. The transformation to β-phase in Si_3N_4 ceramics prepared using the nanosized amorphous Si_3N_4 powder was more greatly promoted than that using submicron-sized α-Si_3N_4 powder.

Acknowledgments This work was performed as Research Fellow of the Japan Society for the Promotion of Science (No.07570).

References

1) M. Tokita, *J. Soc. Powder Technol. Jpn.*, 30, 790–804 (1993).
2) Z. Shen, M. Johnsson, Z. Zhao and M. Nygren, *J. Am. Ceram. Soc.*, 85, 1921–1927 (2002).
3) Y. Zhou, K. Hirao, Y. Yamauchi and S. Kanzaki, *J. Eur. Ceram. Soc.*, 24, 3465–3470 (2004).
4) J. A. Schneider, S. H. Risbud and A. K. Mukherjee, *J. Mater. Res.*, 11, 358–362 (1996).
5) T. Nishimura, M. Mitomo, H. Hirotsuru and M. Kawahara, *J. Mater. Sci. Lett.*, 14, 1046–1047 (1995).
6) M. Suganuma, Y. Kitagawa, S. Wada and N. Murayama, *J. Am. Ceram. Soc.*, 86, 387–394 (2003).
7) J. R. Groza, J. D. Curtis and M. Krämer, *J. Am. Ceram. Soc.*, 83, 1281–1283 (2000).
8) Y. Zhou, K. Hirao, M. Toriyama and H. Tanaka, *J. Am. Ceram. Soc.*, 83, 654–656 (2000).
9) J. Tatami, M. Iguchi, M. Hotta, C. Zhang, K. Komeya, T. Meguro, M. Omori, T. Hirai, M. E. Brito and Y.-B. Cheng, *Key Engineering Materials*, 237, 105–110 (2003).
10) M. Hotta and T. Goto, *J. Ceram. Soc. Japan*, 116, 744–748 (2008).
11) M. Hotta and J. Hojo, *J. Ceram. Soc. Japan*, 117, 1009–1012 (2009).
12) C. P. Gazzara and D. R. Messier, *Am. Ceram. Soc. Bull.*, 56, 777–780 (1977).
13) L. J. Bowen, R. J. Weston, T. G. Carruthers and R. J. Brook, *J. Mater. Sci.*, 13, 341–350 (1978).
14) J. A. Schneider, S. H. Risbud and A. K. Mukherjee, *J. Mater. Res.*, 11, 358–362 (1996).